

Modeling of Supercapacitor

Ganesh Madabattula¹, Sanjeev K. Gupta^{*2}

^{1,2}Indian Institute of Science, Bangalore

*Corresponding author: Dept. of Chemical Engg. IISc, Bangalore, sanjeev@chemeng.iisc.ernet.in

Abstract: Recovering and storing energy of a moving vehicle as it slows down and using it to accelerate the vehicle later can significantly increase fuel efficiencies of automobiles. Low cost batteries available today perform quite poorly in applications that require high (dis)charge currents. Use of adequately designed supercapacitors (SC) in electrical circuits in principle allows present day high energy density batteries to be used effectively, as the momentary burden of high (dis)charge currents is taken up by the supercapacitors.

The high capacitance of supercapacitors is achieved by increasing the surface area offered by the electrodes by choosing appropriate porous material such as activated carbon and by reducing the distance over which electric field is experienced to Debye length by using mobile ions in an electrolyte. Supercapacitors are typically modeled as a complex RC circuit. The parameters of such a model do not easily relate to the physical processes such as movement of ions in micro and meso voids in response to applied electric field and building up of charge in double layer. The present work uses a more fundamental transport process based approach, already available in the literature, to model a SC. In this work, a 1D transport model is developed for a SC with porous activated carbon coated electrodes inserted in an aqueous electrolyte solution. The model considers diffusive and convective movement of ions in a straight narrow channel in response to concentration gradient and local electric field. The governing equations are solved using COMSOL. The model explains variation of anodic and cathodic potentials during (dis)charging, recovery of potential drop during relaxation phase after high rate of discharge, limiting current densities, and effect of electrolyte concentration and diffusivities of ions on dynamics of (dis)charging process. The approximations used to obtain 1D model were dropped and simulations were carried with full 2D domain in COMSOL. The simulation results show that 1D model for a SC is quite adequate.

Keywords: Supercapacitor, double layer capacitance, energy storage, 1D model.

1. Introduction

Supercapacitors (SC) are high power density energy storage devices and are used where batteries alone cannot provide energy needs at high rates. SC's help us in recovering energy from decelerating automobiles, tides and wind etc. and supply energy when there is a momentary demand at high rates. Emergency power backup for computational facilities and aeroplanes and peak power load at rocket launching and automobiles startup are some of the examples. The most widespread use of SC is in hybrid electric automobiles where SC's share peak energy demand and thereby help to extend the battery life. SC's also recover energy while applying brakes, thereby increasing the fuel efficiency of vehicles. In hybrid system, SC gets charged first in a few seconds. It later charges the battery after the energy source is withdrawn.

A typical SC contains two electrodes made up of high surface area activated porous carbon particles coated on a highly conductive current collector. The electrodes are separated by an ion permeable polymer membrane to avoid short circuit. The use of scaling up of SC in commercial hybrid vehicles require 5 Wh/kg energy density, 1 kW/kg power density, a RC time constant <1s and low cost(<US\$2-3/Wh) (Burke, 2000). To meet these requirements, several supercapacitors are connected in series and parallel to form a network. These bundles of SC's have high resistance, time lag, unequal energy distribution and less efficiency. In the present work, we model to an electrochemical supercapacitors with no Faradaic reactions on electrode to under movement of ions in supercapacitors better.

2. Model equations for supercapacitor

Present modeling approach is based on the transport processes used earlier by (Johnson and

Newman (1971), Newman and Thomas-Alyea (2004) and Srinivasan and Weidner (1999) to understand ion pore resistance in a laboratory scale SC. The model uses local concentration dependent ionic conductivity. The electrolyte used is 3M H_2SO_4 solution.

Figure 1 shows the schematic of a laboratory scale SC modelled in the present work. The two sided electrodes have activated porous carbon coated on current collector and inserted in a bulk electrolyte pool. The ion permeable membrane separator is not present, as it is unnecessary for the present setup. The resistance offered by the current collectors is neglected in the model due to their high conductivity.

Figures 2 and 3 show the simplified SC setup for 1D model. The ends in 1D model are connected by assuming continuity of fluxes and values of variables to make the system closed. The capacitor system can thus be separated into two independent capacitors in parallel with different internal resistance for movement of ions on account of different separation distances between inner and outer faces of positive and negative electrodes shown as L_{s1} and L_{s2} in the figures.

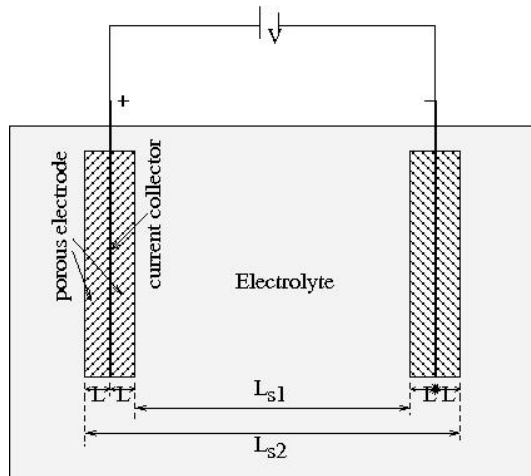


Figure 1: Schematic representation of supercapacitor setup

The total capacitance of the setup is

$$C_T = C_1 + C_2 \quad (1)$$

and

$$\frac{1}{C_1} = \frac{1}{C_{anode,1}} + \frac{1}{C_{cathode,1}} \quad (2)$$

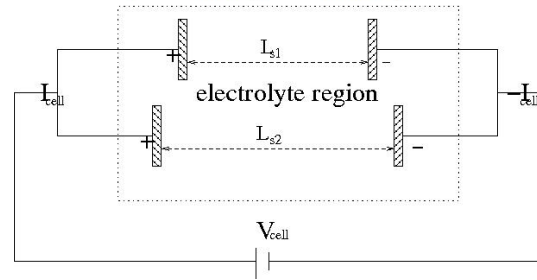
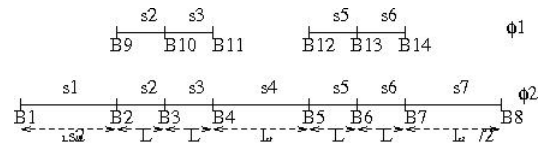


Figure 2: Approximation of two parallel supercapacitors



ϕ_1 is active in porous regions of electrode matrix phase
 ϕ_2 is active in all subdomains
 B1 to B8: boundaries for electrolyte phase
 B9 to B14: boundaries for electrode matrix phase
 L: thickness of one side porous electrode
 subdomains s2, s3: porous regions of one electrode
 subdomains s5, s6: porous regions of other electrode
 subdomain s4: electrolyte region
 subdomain s1, s7: electrolyte regions

Figure 3: 1D model of supercapacitor

$$\frac{1}{C_2} = \frac{1}{C_{anode,2}} + \frac{1}{C_{cathode,2}} \quad (3)$$

2.1 One dimensional concentration dependent model

2.1.1. Porous Electrode Phase

The governing equations scaled with electrode thickness, L ($150e^{-6}m$) are discussed next. The electronic current through electrode (A/m^2), given by Ohm's law is:

$$i_1 = -\frac{\sigma}{L} \frac{\partial \phi_1}{\partial x} \quad (4)$$

where σ is electrode conductivity (S/m).

The charge conservation equation in electrode phase is (Johnson and Newman, 1971)

$$\nabla \cdot (i_1) = -L S_d C_d \frac{\partial (\phi_1 - \phi_2)}{\partial t} \quad (5)$$

where r.h.s represents charge conserved in double layer, with capacitance C_d . The latter is taken to be constant (F/m^2). Here, S_d is interfacial surface area (m^2/m^3).

The current distribution in electrolyte phase in all the subdomains is given by

$$i_2 = F \sum z_i N_i \quad (6)$$

where z_i is valency and N_i is the flux of i^{th} species

The Nernst-Planck equation (without convection) for flux of i is

$$N_i = \left[-z_i u_i F C_i \frac{\partial \phi_2}{\partial x} - \frac{\epsilon D_i}{L} \frac{\partial C_i}{\partial x} \right] \quad (7)$$

The ionic current through electrolyte (A/cm²) (Newman and Thomas-Alyea, 2004) is given by

$$i_2 = -\frac{\kappa_{pn}}{L} \frac{\partial \phi_2}{\partial x} - \frac{F\epsilon}{L} \left(z_+ D_+ \frac{\partial C_+}{\partial x} + z_- D_- \frac{\partial C_-}{\partial x} \right) \quad (8)$$

where first term on the r.h.s represents the flux due to electric field and the second term represents the flux due to the concentration gradient. κ_{pn} is electrolyte conductivity in porous medium, ϵ is porosity of electrode, z_+ and z_- are charge numbers of cation and anion and D_+ and D_- are diffusivities of cation and anion respectively.

The charge conservation equation in electrolyte phase is (Johnson and Newman, 1971)

$$\nabla \cdot i_2 = L S_d C_d \frac{\partial (\phi_1 - \phi_2)}{\partial t} \quad (9)$$

The overall charge balance with the assumption of electroneutrality is (Johnson and Newman, 1971)

$$\nabla \cdot i_2 + \nabla \cdot i_1 = 0 \quad (10)$$

Mass balance equation for i^{th} species is:

$$\frac{\partial C_i}{\partial t} = -\frac{\partial N_i}{\partial x} + R_i \quad (11)$$

where R_i is the source term (double layer contribution) and N_i is the flux, defined as:

$$N_i = \left[-\frac{\epsilon D_{sp}}{L} \frac{\partial C_i}{\partial x} + \frac{t_i^0 i_2}{z_i F} \right] \quad (12)$$

At the negative electrode (subdomains s_5 and s_6)

$$\epsilon L \frac{\partial C_+}{\partial t} = -\nabla \cdot \left[-\frac{\epsilon D_{sp}}{L} \frac{\partial C_+}{\partial x} + \frac{t_+^0 i_2}{z_+ F} \right] + \frac{L S_d C_d}{z_+ F} \frac{\partial (\phi_1 - \phi_2)}{\partial t} \quad (13)$$

$$\epsilon L \frac{\partial C_-}{\partial t} = -\nabla \cdot \left[-\frac{\epsilon D_{sp}}{L} \frac{\partial C_-}{\partial x} + \frac{t_-^0 i_2}{z_- F} \right] \quad (14)$$

At the positive electrode (subdomains s_2 and s_3)

$$\epsilon L \frac{\partial C_-}{\partial t} = -\nabla \cdot \left[-\frac{\epsilon D_{sp}}{L} \frac{\partial C_-}{\partial x} + \frac{t_-^0 i_2}{z_- F} \right] + \frac{L S_d C_d}{z_- F} \frac{\partial (\phi_1 - \phi_2)}{\partial t} \quad (15)$$

$$\epsilon L \frac{\partial C_+}{\partial t} = -\nabla \cdot \left[-\frac{\epsilon D_{sp}}{L} \frac{\partial C_+}{\partial x} + \frac{t_+^0 i_2}{z_+ F} \right] \quad (16)$$

where t_{o+} and t_{o-} are transference numbers of positive and negative ions, which accounts for fraction of current carried by positive and negative ions.

$$t_+^0 + t_-^0 = 1 \quad (17)$$

The second term on the r.h.s. of equation for C_i accounts for charge accumulation near electrode surface due to the formation of double layer while charging and discharging.

The salt concentration is given by

$$C_s = \frac{C_+}{\nu_+} = \frac{C_-}{\nu_-} \quad (18)$$

2.1.2 Bulk electrolyte phase

The concentration variation of ions in subdomains s_1 , s_4 and s_7 is given by

$$L \frac{\partial C_+}{\partial t} = -\nabla \cdot \left[-\frac{D_{ss}}{L} \frac{\partial C_+}{\partial x} + \frac{t_+^0 i_2}{z_+ F} \right] \quad (19)$$

$$L \frac{\partial C_-}{\partial t} = -\nabla \cdot \left[-\frac{D_{ss}}{L} \frac{\partial C_-}{\partial x} + \frac{t_-^0 i_2}{z_- F} \right] \quad (20)$$

$$i_2 = -\frac{\kappa_{sn}}{L} \frac{\partial \phi_2}{\partial x} - \frac{F}{L} (z_+ D_{+0} \frac{\partial C_+}{\partial x} + z_- D_{-0} \frac{\partial C_-}{\partial x}) \quad (21)$$

where κ_{sn} is conductivity of the electrolyte in bulk. As the charge accumulation in the bulk is zero,

$$\nabla \cdot i_2 = 0 \quad (22)$$

2.1.3 Initial conditions

The initial values for variables C_+ and C_- are:

$$C_+ = C_{s0} \nu_+ \quad C_- = C_{s0} \nu_-$$

2.1.3.1 Discharge cycle

At positive electrode, $\phi_1=1$. At negative electrode, $\phi_1=0$. Everywhere in the supercapacitor, $\phi_2 = 0.5$.

2.1.3.2 Charge cycle

At positive electrode, $\phi_1=0$. At negative electrode, $\phi_1=0$. Everywhere in the supercapacitor, $\phi_2 = 0$.

2.2 Boundary conditions

The model consists of seven subdomains involving 25 independent equations for two potentials ϕ_1 and ϕ_2 and two concentrations C_+ and C_- . The system of equations requires 50 independent boundary relations to completely

specify the model. These relations are discussed next.

Boundaries B_3 and B_6 where current collectors are located act as barrier to the movement of ions, hence i_2 and N_i become zero at these locations.

At boundaries B_9 , B_{11} , B_{12} and B_{14} , porous electrode face is in contact with the bulk electrolyte. It is assumed that the surface area offered at these surfaces is negligible compared to the interior surface, hence no current flows in the matrix phase at these locations ($i_1 = 0$).

At boundaries B_2 , B_5 , B_4 and B_7 where electrolyte in porous electrode face meets bulk electrolyte, continuity conditions require both fluxes (N_i and i_2) and absolute values (ϕ_2 , C_+ , and C_-) to be equal on both sides. These boundaries are continuous in ionic current flow. At boundary B_{10} , where cell current I_{cell} is drawn (from the positive electrode during discharge)

$$i_1|_R - i_1|_L = -I_{cell} \quad (23)$$

$$\phi_1|_L = \phi_1|_R \quad (24)$$

At boundary B_{13} , where cell current is pumped (into the negative electrode during discharge)

$$i_1|_R - i_1|_L = I_{cell} \quad (25)$$

$$\phi_1|_L = \phi_1|_R \quad (26)$$

Equations 23 and 25 represent jump conditions for flux at the respective boundaries, physically they represent a SC discharging at current I_{cell} . Electrons equivalent to current I_{cell} are withdrawn on one electrode and pumped into the other. The direction of movement of electrons is reversed during the charging process.

At boundaries B_1 and B_8 , symmetric boundary condition is applied: ϕ_2 and C_i at B_8 is equal to ϕ_2 and C_i at B_1 , and the ionic flux leaving one boundary enters through the other. One more equation is required to completely specify the problem, and it is given by

$$\phi_1 = 0 \quad (27)$$

at B_{14} . Equation 27 serves as a reference point for all the potentials in the supercapacitor.

2.3 Two dimensional model

The geometry for 2D model is similar to the one shown in Figure 1. The 2D model equations were developed based on 1D model. The initial and the boundary conditions for the simulations are the same as those for the 1D problem. The periodicity b.c. used in 1-d model is not required as the entire geometry is taken into account. Cell current boundary conditions are applied to entire current collector plate (A/m^2) and reference potential $\phi_2 = 0$ is specified at the top of current collector of negative electrode.

2.4 Parameters used in the model

In the simulations, it was assumed that electrolyte is asymmetric (not binary). H_2SO_4 is an example for asymmetrical electrolyte. It dissociates into two H^+ cations and one SO_4^{2-} . So, concentration change at both electrodes is not the same as that in the case of symmetrical electrolyte, further both the ions have different diffusivities and ionic sizes. Diffusivity of electrolyte in bulk medium is given by (Newman and Thomas-Alyea, 2004)

$$D_{s0} = \frac{D_{+0}D_{-0}(z_+ - z_-)}{z_+D_{+0} - z_-D_{-0}} \quad (28)$$

Diffusivity of i^{th} ion in any porous medium

$$D_i = D_{i0}\epsilon^{0.5} \quad (29)$$

where ϵ is porosity of given subdomain.

Diffusivity of salt in bulk electrolyte

$$D_{ss} = D_{s0}\epsilon_s^{0.5} = D_{s0} \quad (30)$$

where $\epsilon_s = 1$ for bulk electrolyte.

Diffusivity of salt in porous medium (Newman and Thomas-Alyea, 2004),

$$D_{sp} = D_{s0}\epsilon^{0.5} \quad (31)$$

where ϵ is porosity of the medium.

Conductivity of electrolyte in porous electrode is given as (Bruggeman empirical relation),

Table 1: Parameters used in simulating the model

Parameter	Value	Reference
C_d	3×10^{-5} F/cm ²	Johnson and Newman (1971)
C_s	3 M	assumed
D_{+0}	9.312×10^{-5} cm ² /s	Newman and Thomas-Alyea (2004)
D_{-0}	1.065×10^{-5} cm ² /s	Newman and Thomas-Alyea (2004)
I_{cell}	1 A/cm ²	assumed
L	150 μ m	assumed
L_s	600 μ m	assumed
L_{s2}	1200 μ m	assumed
S_d	3×10^6 cm ² /cm ³	Johnson and Newman (1971)
T	298 K	assumed
σ	10^5 S/cm	Lin <i>et al.</i> (2002)
ϵ	0.25	Johnson and Newman (1971)
ϵ_s	1	no separator

$$\kappa_{pn} = \kappa_{p0} \epsilon^{1.5} \quad (32)$$

Where κ_{p0} , the conductivity of electrolyte in bulk medium in the context of dilute solution theory (Newman and Thomas-Alyea, 2004), is given by

$$\kappa_{p0} = F^2 \sum_i \frac{z_i^2 D_{i0} C_i}{RT}, (i = +, -) \quad (33)$$

$$\kappa_{sn} = \kappa_{p0} \quad (34)$$

3. Results and discussion

The models discussed in the previous sections are simulated using COMSOL Multiphysics (v4.2a), with multiphysics (PDE coefficient) and AC/DC (electric current (ec)) modules.

3.1 1D results

The domain considered for 1D modeling spans 28 units. Thickness of the porous electrode on one side of the current collector represents one unit (L). This geometry was meshed to 3500 elements. Further refinement of the mesh did not

change the simulation results. Solver used is 'Direct(PARDISO)' with flexibility to take time steps on its own. Ends of the domain are connected with periodic boundary condition (PBC) to maintain continuity of fluxes and variables.

Using the concentration dependent model, the galvanostatic discharge curve (V_{cell} vs t) obtained at 1 A/m² and 3M H₂SO₄ solution is shown in figure 4. The SC is initially charged to 1V. Figure 4 shows that there is sudden potential drop followed by a slow linear decrease. The reason for this behavior is the resistance offered to ions in the electrolyte. This discharge curve profile is in qualitative agreement with the actual SC with assumptions used for simulations. These result are consistent with

$$tI_{cell} = S_d C_d 2L (V_{cell}/2) \quad (35)$$

The amount of charge recovered for 1 A/cm² is less than given by equation 35 due to the resistance offered by the electrolyte, it can be recovered though after the capacitor is allowed to relax.

Figure 4 also shows anode and cathode potentials at 1 A/cm² discharge current and 3M electrolyte concentration. These potentials are computed by introducing a reference point in the center of SC, i.e. in between the inner faced electrodes.

These potentials are expressed as

$$V_a = \phi_{2,r} - \phi_{1,-} \quad (36)$$

$$V_c = \phi_{1,+} - \phi_{2,r} \quad (37)$$

$$V_{cell} = V_c - V_a \quad (38)$$

where V_a is anode potential, V_c is cathode potential and V_{cell} is cell potential. $\phi_{1,+}$, $\phi_{1,-}$ are potentials of positive and negative electrodes respectively. $\phi_{2,r}$ is potential of reference point. After $t=1.3$, the cell was left to relax after discharge (see Figure 4). During this period, the unrecovered charge helps in raising the potential.

The potential difference ($\phi_1 - \phi_2$) between the electrode and the electrolyte at an interface is

an indication of the extent of charge present at the latter. These profiles at 1 A/cm^2 , 3M are shown in Figure 5. Initially, $\phi_1 - \phi_2$ profiles are flat. The non uniform potential difference profiles shown for $t=0.02\text{s}$ represents the spatially non uniform charge distribution at the interface in the electrode. The figure shows that $\phi_1 - \phi_2$ profiles approach zero as the SC discharges. This kind of non uniform discharge of electrode is not observed at low currents, say 0.1 A/cm^2 because the electrolyte resistance does not dominate, and therefore does not accumulate leading to full recovery of charge stored in SC.

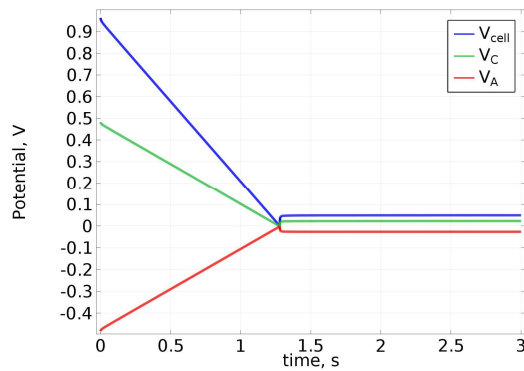


Figure 4: Cell voltage, anodic and cathodic potential profiles during discharge and relaxation at 1 A/cm^2 , 3M .

The concentration profiles during discharge at 1 A/cm^2 and 3M initial concentration are shown in Figure 6. The aqueous electrolyte used in SC dissociates into H^+ and SO_4^{2-} . Cations, H^+ have nine times higher diffusivity than anions, SO_4^{2-} .

The electroneutrality constraint tells that at any point in space

$$C_+ = C_s \nu_+ \quad (39)$$

$$C_- = C_s \nu_- \quad (40)$$

$$\sum z_i C_i = 0 \quad (41)$$

To maintain this condition, H^+ ions released at the negative electrode approach the positive electrode faster than the approach of SO_4^{2-} ions released on positive electrode to negative electrode. This manifests through difference in peak heights of salt concentration (C_s) at both electrodes as shown in Figure 6.

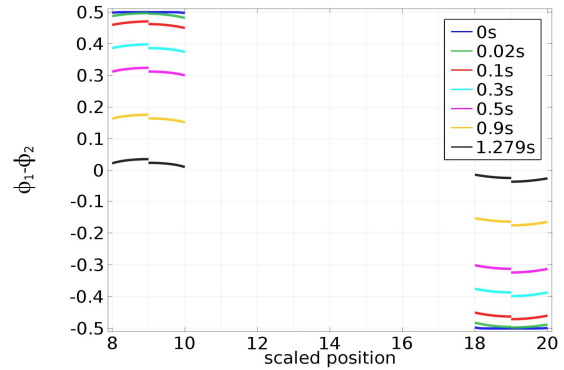


Figure 5: Potential difference profiles across the double layer in porous electrode at 1 A/cm^2 , 3M .

3.2 2D results

The transport parameters required in the model are assumed to be isotropic. COMSOL Multiphysics is used. The dimensions of geometry of SC is taken is 20×12 after scaling the space coordinate with L , the thickness of the porous electrode coated on one side of current collector. The electrodes of size 2×8 are placed at the top of the supercapacitor at coordinates (5,12) and (15,12) (Figure 1). This geometry is meshed into 15406 triangular elements, 840 edge elements and 29 vertex points. The solver used to solve the system of equations are "Direct(PARDISO)" and the relative tolerance is taken as 10^{-5} . Figure 7 shows the comparison of galvanostatic discharge curves of SC at 1 A/cm^2 and 3M initial electrolyte concentration. The result obtained for 2D are close to those obtained with 1D as shown in Figure 7. Though they are not exact, differences are minimum.

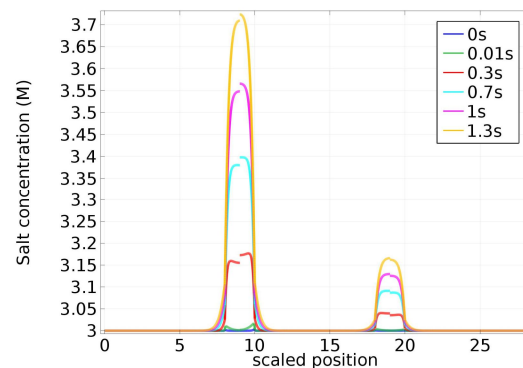


Figure 6: Concentration variation profiles during discharge at 1 A/cm^2 , 3M

The assumption made in 1D, i.e. L_{s2} , the space between outer faced electrodes is double of the inner space (L_{s1}) is need to be extended to account for more resistance.

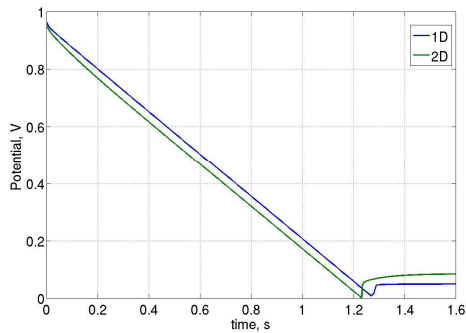


Figure 7: Comparison of discharge profiles from 2D and 1D simulations at 1 A/cm^2

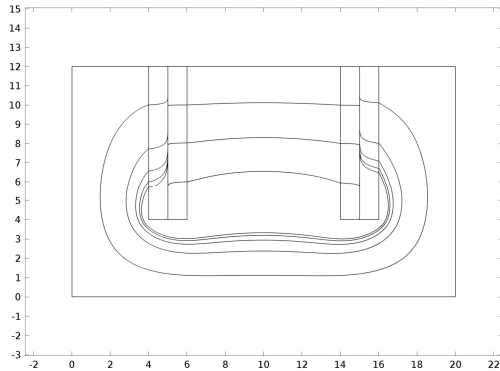


Figure 8: Gradient of electrolyte potential streamlines at 1 A/cm^2 , 3M

Figure 8 shows the streamlines of gradients of ionic flux of x-component, ϕ_{2x} and y-component, ϕ_{2y} . The figure shows that streamlines of potential gradients of inner faced and outer faced electrodes are quiet independent of each other. The major assumption made in 1D model which considered electric field between the outer faced and the inner faced electrodes separately draws support from the 2-D results shown in the figure. The phenomenon of potential recovery after discharge is the same as that for 1D. Figure 7 shows recovery in potential after discharge at 1 A/cm^2 and 3M .

4. Conclusion

In this work, a 1D concentration dependent model is developed for laboratory scale two electrode aqueous electrolyte double layer

capacitor, that doesn't involve any Faradaic processes. This model, based on the transport approach, is built from the first principles of ionic movement. Using the isotropic transport properties, 2D model equations were also developed. The 2D model does not require the assumption of periodicity made in the 1D model and is more realistic. A comparison of both 1D and 2D model prediction shows that the approximation made in developing 1D model are valid.

The simulation results show that both the models explain recovery of potential during relaxation after dis(charge) and its dependence on current and concentration, and the failure of SC during charging at high currents and low concentrations of electrolyte. The models also explain galvanostatic discharge curves, relative utilization of charge, process of double layer formation and its disappearance.

8. References

1. Burke, A. (2000) Ultracapacitors: why, how, and where is the technology. *Journal of power sources* **91**(1), 37–50.
2. Johnson, A. and Newman, J. (1971) Desalting by means of porous carbon electrodes. *Journal of the Electrochemical Society* **118**, 510.
3. Lin, C., Popov, B. and Ploehn, H. (2002) Modeling the effects of electrode composition and pore structure on the performance of electrochemical capacitors. *Journal of the Electrochemical Society* **149**, A167.
4. Newman, J. and Thomas-Alyea, K. (2004) *Electrochemical systems*. Wiley-Interscience.
5. Srinivasan, V. and Weidner, J. (1999) Mathematical modeling of electrochemical capacitors. *Journal of the Electrochemical Society* **146**, 1650–1658.